TECHNICAL RATIONALE FOR METAL FUEL IN FAST REACTORS

YOON IL CHANG
Argonne National Laboratory
9700 S. Cass Avenue Argonne, IL 60439
E-mail : YChang@anl.gov

Received April 13, 2007

Metal fuel, which was abandoned in the 1960's in favor of oxide fuel, has since then proven to be a viable fast reactor fuel. Key discoveries allowed high burnup capability and excellent steady-state as well as off-normal performance characteristics. Metal fuel is a key to achieving inherent passive safety characteristics and compact and economic fuel cycle closure based on electrorefining and injection-casting refabrication.

KEYWORDS : Fast Reactor, Metal Fuel, Inherent Safety, Pyroprocessing

1. INTRODUCTION

Metal fuel was the original choice in early fast reactors (EBR-I, EBR-II, Fermi-1, and Dounreay Fast Reactor) because it is compatible with the liquid metal sodium coolant. The metal fuel development as fast reactor fuel was abandoned in the late 1960's in favor of ceramic oxide fuel developed for the commercial water cooled reactors. At that time, it was perceived that metal fuel could not achieve high burnup because the irradiation induced swelling could not be constrained by cladding.

However, EBR-II continued to use metal fuel as its driver fuel and its burnup capability was drastically improved through discoveries in the late 1960's and irradiation experience in the 1970's.[1-3] The key discovery was that metallic fuel can achieve high burnup by allowing room for fuel to swell rather than trying to constrain the swelling. The fuel swelling is driven primarily by the internal pressure of fission gas bubbles. Once fuel swells by about 30% in volume, then the fission gas bubbles interconnect and provide passage for fission gas to be released to the plenum located above the fuel rod. By adequately sizing the plenum to contain fission gases released through interconnected porosity, the fuel swelling can be easily constrained by the cladding and a high burnup can be easily achieved. The porosity would also be available to accommodate the inexorable swelling from the accumulation of solid fission products.

A schematic of metal fuel is shown in Fig. 1. The fuel slug is loaded inside the cladding, and the gap between the slug and cladding is filled with sodium which acts as thermal bond until fuel swells out to the cladding. The fuel slug can be in full length or segmented pieces loaded on top of each other.

The original EBR-II Mark-I metal fuel pin was designed with 85% smear density. With the discovery on fuel swelling, the Mark-II fuel design incorporated 75% smear density. The burnup was gradually increased and bulk of Mark-II design achieved 7-8% burnup. The Mark-II cladding also had an indentation above the fuel column to act as a fuel restrainer. The original indentation was a chisel shape, which became a weak point at about 8% burnup. However, with a new cladding design that changed from a chisel to a spherical indent, much higher burnup could be achieved and some fuel pins reached 18.5% burnup. Over 40,000 Mark-II metal fuel pins have been successfully irradiated through early 1980's.

The EBR-II Mark-I and Mark-II fuels are composed of 95% uranium and 5% fissium alloy. During the first 5 years of EBR-II operation, the fuel was recycled through melt-refining and injection casting refabrication.[4] In this early pyrometallurgical processing, noble metal fission products were recycled back along with the recovered uranium. The equilibrium composition through repeated recycle was approximately as follows:

Molybdenum	2.46%
Ruthenium	1.96%
Rhodium	0.28%
Palladium	0.19%
Zirconium	0.10%
Niobium	0.01%
Total	5.00%

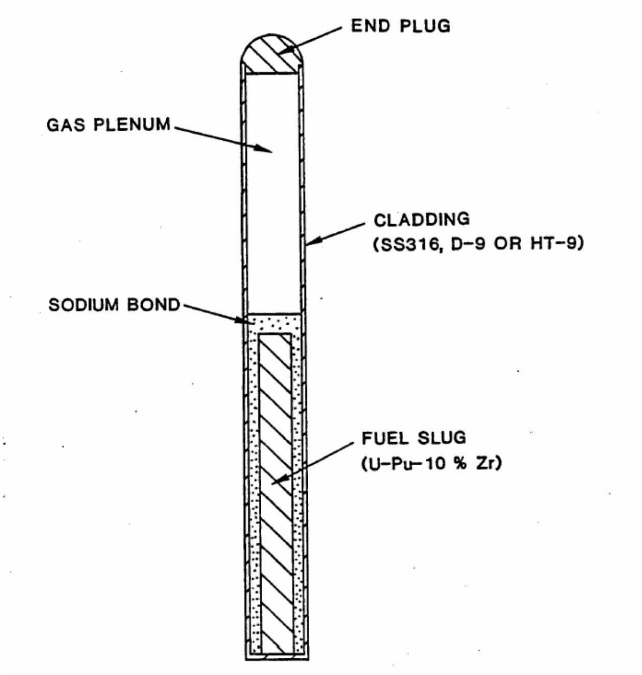

Fig. 1 Schematic of Metallic Fuel Pin

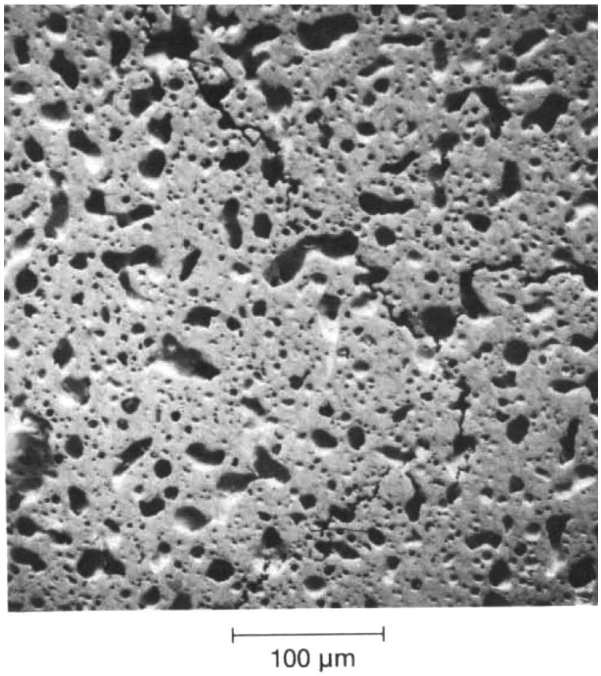

Fig. 2 Fission Gas Pore Morphology of Irradiated U-10Zr Fuel

This composite alloy was called "fissium." Because of their beneficial effects on the metal fuel irradiation performance characteristics, the 5% fissium addition was continued for all Mark-I and Mark-II fuels even after the recycle operation ceased in 1969.

2. STEADY-STATE IRRADIATION PERFORMANCE

When the Integral Fast Reactor (IFR) Program [5-6] was initiated in 1984, a 10% zirconium addition, replacing 5% fissium, was selected as the reference alloying agent for both uranium and plutonium bearing fuels. Earlier irradiation tests of various alloys indicated that Zr exhibited exceptional compatibility with cladding in addition to significantly increasing the fuel alloy solidus and fuel-cladding eutectic temperatures. Therefore, as the Mark-II driver fuel assemblies reached their irradiation limits, the EBR-II core was gradually converted with new Mark-III fuel based on U-10%Zr with D-9 or SS-316 cladding. Later, Mark-IV fuel with HT-9 cladding was introduced.

At the same time, Experimental Fuels Laboratory (EFL) was established in 1984 to fabricate plutonium-bearing ternary fuel, U-Pu-10%Zr. A total of 16,811 U-Zr and 660 U-Pu-Zr fuel pins were irradiated in EBR-II in the next 10 years until EBR-II was permanently shut down at the end of September, 1994.

The irradiation behavior of the zirconium alloy metal fuel is very similar to that of the U-fissium. The fission gas pore morphology of the irradiated U-10Zr fuel is illustrated in Fig. 2. The dark areas represent pores, which tend to get interconnected allowing fission gas release to the plenum. Maintaining the fuel smeared density below 75% is crucial to have the interconnected porosity.

In high plutonium ternary fuel, constituent redistribution occurs in early stage of irradiation and radial fuel zones are formed. The constituent migration is driven primarily by temperature gradient, and hence it is predominantly radial redistribution. Zirconium tends to migrate to the center and the periphery, and uranium migrates in the opposite direction. Plutonium on the other hand tends to stay put. This is fortuitous and tends to help the performance issues in that Zr moves to the center raising the solidus temperature at peak temperature region and to the periphery helping the fuel-cladding compatibility.

This radial zone formation occurs rapidly in early stage of irradiation and it enhances the radial swelling markedly. This high rate of radial swelling creates stresses in the peripheral fuel large enough to result in some crack formation. The large cracks will eventually get filled with fuel as irradiation continues. This anisotropic swelling then results in much smaller axial growth of the ternary fuel compared to U-fissium or U-Zr fuels. The axial growth of the uranium based fuel is in the range of 8-10%, whereas it is in the range of 3-4% for the ternary fuel.

In spite of the fuel restructuring, the metallic fuel has demonstrated excellent steady-state irradiation performance characteristics. In addition to the 30 years of extensive

Table 1. Metal Fuel Irradiation Tests in EBR-II

Assembly ID	Description	Cladding Type	Pin OD mm	Pu content % HM	Burnup at.%
X419	Lead test	D9	5.8	0/8.9/21.1	12.0
X420	Lead test	D9	5.8	0/8.9/21.1	17.1
X421	Lead test	D9	5.8	0/8.9/21.1	18.4
X423	Lead test	SS316	7.4	0/3.3/8.9/21.1/24.4/28.9	5.0
X425	IFR lead test	HT9	5.8	0/8.9/21.1	19.3*
X427	Run beyond eutectic	SS316	4.4	0	11.5
X429	Fabrication variable I	HT9/SS316	5.8	0/8.9/21.1	14.4
X430	Advanced HT9 test	HT9	7.4	0/21.1/24.4/28.9	11.5*
XY-24	RBCB high Pu	SS316	4.4	0/21.1	7.6
XY-27	RBCB medium Pu	SS316	4.4	0/8.9	6.6
X397	Advanced metal blanket	D9	12.9	0	2.0
X431	HT9 blanket test	HT9	9.4	0	3.8*
X432	HT9 blanket test	HT9	9.4	0	4.4*
X435	Mk-III qualification	D9	5.8	0	19.9*
X436	Mk-III qualification	D9	5.8	0	9.3
X437	Mk-III qualification	D9	5.8	0	10.3
X438	Mk-III qualification	D9	5.8	0	9.9
X441	Variable Zr: 6/10/12%	HT9/D9	5.8	21.1	12.7
X447	Mk-III high temperature	HT9/D9	5.8	0	10.1
X448	Mk-IV qualification	HT9	5.8	0	14.8*
X449	Mk-IV qualification	HT9	5.8	0	11.3
X450	Mk-IV qualification	HT9	5.8	0	10.2
X451	Mk-IV qualification	HT9	5.8	0	13.8*
X452	Fuel impurities	D9	5.8	0	6.1
X453	Fuel impurities	D9	5.8	0	8.5
X454	Fuel impurities	D9	5.8	0	9.0
X455	Fuel impurities	D9	5.8	0	9.0
X481	Pu feedstock	SS316	5.8	21.1	9.0
X482	RBCB high Pu	D9	5.8	21.1	13.5
X483	Mk-IIIA qualification	SS316	5.8	0	15.0*
X484	Mk-IIIA qualification	SS316	5.8	0	11.7
X485	Mk-IIIA qualification	SS316	5.8	0	10.5
X486	Mk-IIIA qualification	SS316	5.8	0	13.9*
X489	High Pu compatibility	HT9/HT9M	5.8	21.1/31.1	5.4*
X492	Zr sheath	SS316	5.8	0/21.1	10.5*
X496	Long life	HT9	6.9	0	8.3*
X501	Actinide burner	HT9	5.8	0/22.2	5.9*
X510	Metal fuel source pin	HT9	5.8	0/22.2	1.9*
X521	Synthetic LWR fuel	HT9	5.8	0/22.2	1.9*

*Still under irradiation when EBR-II was permanently shut down

irradiation experience with the driver fuel in EBR-II, extensive U-Zr and U-Pu-Zr irradiation tests have been conducted as part of the IFR Program, which is summarized in Table 1. The IFR Program test matrix included various combinations of cladding materials (SS316, D-9, HT-9, and HT-9M), pin diameters (4.4, 5.8, 6.9, 7.4, 9.4, and 12.9 mm), plutonium concentrations (3.3, 8.9, 21.1, 24.4, 28.9, and 31.3% of heavy metal), Zr contents (6, 10, and 12%), fuel smeared densities (70, 75, and 85%), fabrication varables (fuel impurity levels), and operating conditions (peak linear power, cladding temperatures, etc.).

Typically, the test assemblies were reconstituted to allow post-irradiation examinations at various burnup levels, and the burnup levels presented in Table1 are peak values achieved. Furthermore, the burnup values with asterisks in Table 1 denote test assemblies that were planned for further irradiation when the EBR-II was shut down on September30, 1994. For example, the X425 lead test with U-Pu-Zr ternary fuel achieved 19.3% burnup and X435 Mk-III driver qualification test achieved 19.9% burnup when the EBR-II was shut down. At the time, there was no indication that these tests needed to be terminated and much higher burnup levels could have been achieved if irradiation continued.

There is a perception that this excellent performance experience of the metal fuel in EBR-II was due to a small pin size (4.4 mm diameter and 34.3 cm length), and there is a concern whether the metallic fuel can perform as well in full length pin expected in commercial fast reactors. However, this fuel length effects were satisfactorily resolved in the FFTF tests. Seven full assemblies of metallic fuel were irradiated in FFTF, as summarized in Table 2. One assembly contained U-Pu-Zr fuel pins, which achieved a peak burnup of 10.2%. The other six assemblies were part of the core conversion qualification tests of U-Zr fuel with HT-9 cladding. All of these assemblies achieved peak burnup in excess of 10% and the lead test achieved a peak burnup of 16%. The FFTF core conversion with metallic fuel was abandoned when a decision was made to shut down FFTF.

The potential performance issues included the effect of height and weight of the long fuel column on fission gas release, fuel swelling characteristics, and potential fuel-cladding mechanical interaction at lower part of the fuel column. The post-irradiation examinations of the FFTF tests indicated that the fission gas release to plenum was comparable to the EBR-II fuel, no difference in constituent migration, axial growth was as predicted, and there was no evidence of enhanced fuel-cladding mechanical interaction.

3. OFF-NORMAL PERFORMANCE CHARACTERISTICS

Metal fuel has excellent transient capabilities. The metal fuel itself does not impose any restrictions on transient operations or load-following capabilities. The robustness of metal fuel is illustrated by the following sample history of a typical driver fuel irradiated during the EBR-II inherent passive safety tests conducted in 1986:

- 40 start-ups and shutdowns
- 5 15% overpower transients
- 3 60% overpower transients
- 45 loss-of-flow (LOF) and loss-of-heat-sink tests including a LOF test from 100% power without scram.

Metal fuel also has benign run beyond cladding breach (RBCB) performance characteristics. As shown in Fig. 3 for the oxide fuel (9% burnup) RBCB test, the initial breach site is widened due to fuel-cladding mechanical interaction caused by low density sodium-fuel interaction product, $Na_3(PuU)O_4$, which results in a small amount of fuel loss to the coolant.

A RBCB test with metal fuel (12% burnup) is illustrated in Fig. 4. Because metal fuel is compatible with sodium, there is no reaction product and the fuel loss is practically zero. The post-irradiation examination shown in Fig. 4 is after operation in RBCB mode for 169 days and there is no indication of breach site enlargement. In another test, metal fuel operated 223 days beyond cladding breach,

Table 2. Metal Fuel Irradiation Tests in FFTF

Assembly ID	Description	CladdingType	Pin OD in.	Pu content % HM	Burnup at.%
IFR-1	Lead test	D9	6.9	0/8.9/21.1	10.2
MFF-1	Driver qualification	HT9	6.9	0	10.0
MFF-2	Driver qualification	HT9	6.9	0	15.9
MFF-3	Driver qualification	HT9	6.9	0	16.0
MFF-4	Driver qualification	HT9	6.9	0	14.8
MFF-5	Driver qualification	HT9	6.9	0	11.4
MFF-6	Driver qualification	HT9	6.9	0	11.0

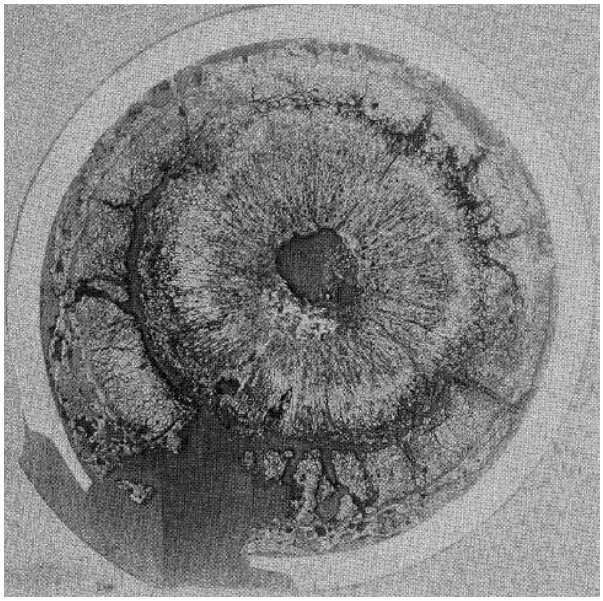

Fig. 3 Oxide Fuel (9% burnup) RBCB Test

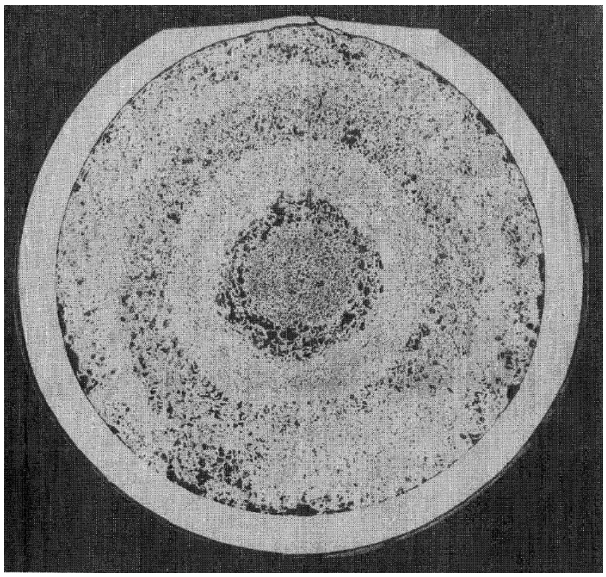

Fig. 4 Metal Fuel (12% burnup) RBCB Test

including many start-up and shut-down transients, and the breach site remained small. Metal fuel is expected to be very reliable. However, even if unforeseen fuel failure occurs, the failed fuel pins could be left in the core until the end of life without raising any operational or safety concerns.

The eutectic formation temperature between the fuel and the cladding has been considered a critical parameter for the metal fuel pin design. The onset of fuel-cladding eutectic formation starts at 700-725°C range, depending on the fuel alloy and cladding types. However, at this onset temperature, not much interaction occurs. In fact, even at 100°C above the eutectic temperature, the eutectic penetration into the cladding is minimal in one hour. Only at much higher temperatures, close to the fuel melting point itself, the eutectic penetration into cladding becomes rapid. Therefore, the eutectic formation is not a primary safety concern during transient overpower conditions. However, the eutectic temperature limits the coolant outlet temperature to 500-510°C in order to provide adequate margins to onset of eutectic formation.

4. INHERENT PASSIVE SAFETY POTENTIAL

Although the metal fuel melting temperature is much lower than that of oxide fuel, it is also much more difficult to raise the fuel temperature because of the high thermal conductivity (~20 W/mK for metal compared to ~2 W/mK for oxide). As a result, operating margins in terms of power can, in fact, be greater for the metal core than for oxide.

Metal fuel provides better or equal safety characteristics across the entire spectrum from normal behavior to postulated severe accidents. However, it is in the inherent passive safety characteristics under the generic anticipated transient without scram events, such as loss-of-flow without scram (LOFWS), loss-of-heat-sink without scram (LOHSWS), and transient overpower without scram (TOPWS), that the metal fuel shows its greatest advantages over oxide fuel.

The inherent passive safety potential of the metal fuel was demonstrated by two landmark tests conducted in EBR-II on April 3, 1986.[7-8] These tests, LOFWS and LOHSWS, demonstrated that the unique combination of the high heat conductivity of metal fuel and the thermal inertia of the large sodium pool can shut the reactor down during these potentially very severe accident situations, without depending on human intervention or the operation of active, engineered components.

The LOFWS event can be initiated by station blackout. Nuclear power plants have redundant power supply sources and even if the alternate line is also disabled, then emergency power supply system on-site will be activated. When this attempt is failed, the plant protection system will automatically shut the reactor down. Of course, the plant protection system has redundancy – if the primary shutdown system fails, then the secondary shutdown system will be activated. All else fails, the operator can manually shut the reactor down. The LOFWS test in EBR-II simulated an ultimate scenario where all of the above safety systems and operator actions had failed.

As the power to the primary pump is lost, the coolant flow is reduced rapidly while the reactor is at its full power. This then causes the reactor coolant outlet temperature rise very rapidly (about 200°C in 30 seconds). This rising coolant temperature then causes the heatup and thermal expansion of the core components, in particular the fuel assembly hardware, which enhances the neutron leakages and hence slowing down the chain reaction. Due to this negative reactivity feedback, the reactor power is shut down all by itself and the coolant temperature rise stops, eventually brought to an asymptotic temperature at equilibrium with the natural heat loss from the system. The predicted coolant outlet temperature responses during the LOFWS test is compared with the actual data taken during the test in Fig. 5, showing excellent agreements. It should be pointed out that during the initial tens of seconds, the mechanical pump inertia provided a flow coastdown avoiding immediate local sodium boiling and enabling a gradual transition to natural convection flow through the core.

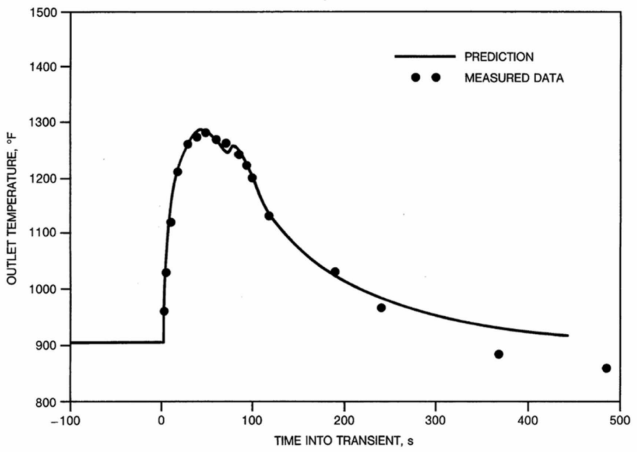

Fig. 5 Loss-of-flow Without Scram Test in EBR-II Demonstrated the Benign Behavior Predicted

Following the LOFWS test, the loss-of-heat-sink without scram test was conducted on the same day. The loss-of-heat-sink was initiated by the shutdown of the intermediate pump, which isolated the primary system, while the primary pump was functioning to remove the heat from the core to the primary tank. The intermediate loop flow is reduced to zero, which disables the normal heat sink in the balance of plant. The core heat is dumped to the entire inventory of the primary sodium, which raises the core inlet temperature. This is a rather slow transient and it took about 10 minutes to raise the primary sodium temperature by about 40°C. This gradual increase in the reactor inlet temperature has the same effect – thermal expansion and enhanced neutron leakages – and the power is reduced. And the reactor outlet temperature is reduced accordingly. The reactor inlet and outlet temperatures are plotted in Fig. 6, comparing the prediction and the actual measured data during the test.

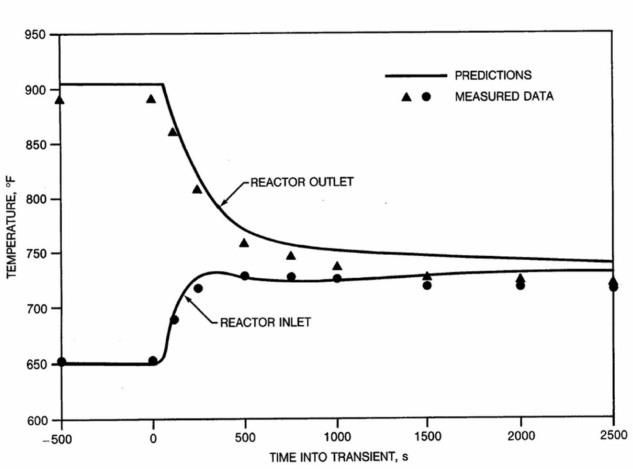

Fig. 6 Reactor Inlet and Outlet Temperature Responses to Loss-of-heat-sink Without Scram Test

These remarkable inherently passive benign responses to the most severe accident scenarios are unique to the metal fueled fast reactor due to the combination of the following three factors:

- Sodium coolant with large margins to boiling temperature,
- Pool configuration with large thermal inertia, and
- Metal fuel with low stored Doppler reactivity.

The first point is obvious to ride out the initial coolant temperature rise. The second point is necessary to provide time for thermal expansion of heavy structures to take place. The third point on metallic fuel is not so obvious and requires some explanation. The characteristics of the negative reactivity feedback caused by the increase in coolant temperature determine the reactor response. The most important factor differentiating the responses in metal and oxide fuels is the difference in stored Doppler reactivity between the two fuel types. As the power is reduced, the stored Doppler reactivity comes back as a positive contribution, tending to cancel the negative feedback due to the structural expansion. The high thermal conductivity of metal fuel and consequent low fuel operating temperature give a stored Doppler reactivity that is only a small fraction of overall negative reactivity feedback. As a result, the power is reduced rapidly. In contrast, oxide fuel has a much greater stored Doppler reactivity (primarily due to higher fuel temperatures rather than the difference

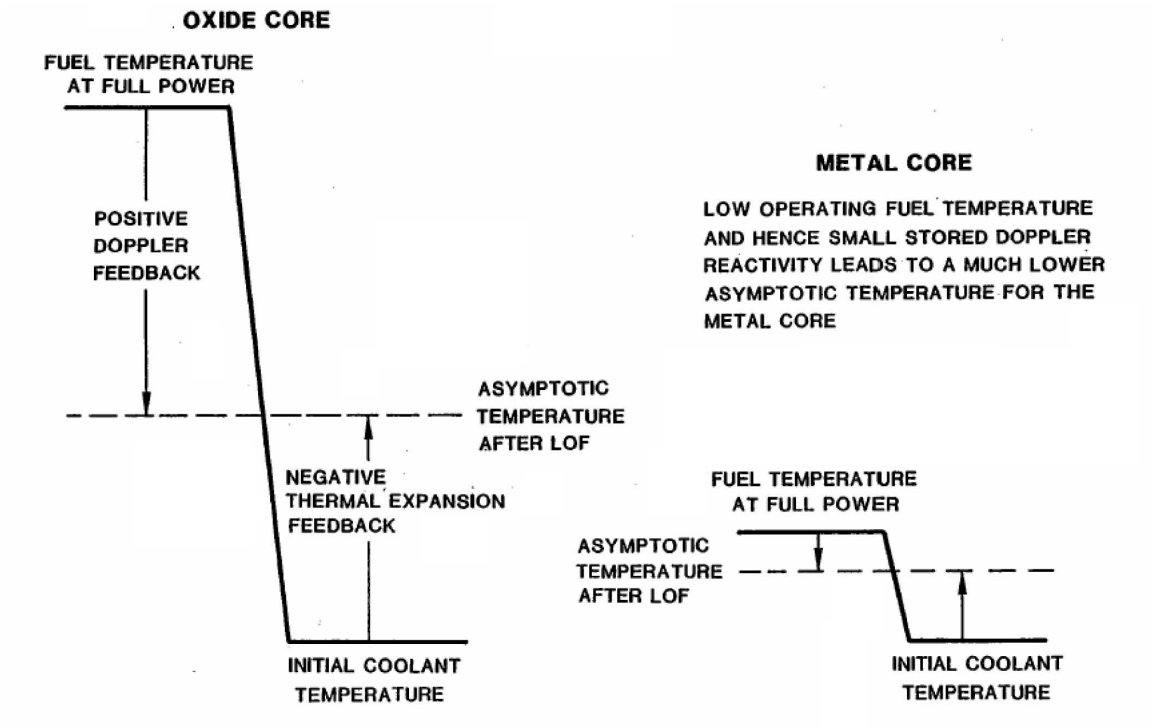

Fig. 7 Asymptotic Temperature Reached during LOFWS Event is Determined by Reactivity Balance: Comparison of Oxide and Metal Cores

in the Doppler coefficient itself), and the power does not decrease rapidly during the LOFWS event. And when the power has been reduced to decay heat levels to counter the stored Doppler reactivity, the coolant temperature maintains a much higher value in an oxide core. This comparison between oxide and metal cores is illustrated schematically in Fig. 7.

The superior neutronics performance characteristics of metallic fuel allow core designs with minimum burnup reactivity swing even for small modular designs. This can be used not only in extending core life to 30 years but also in reducing the TOPWS initiator caused by an unprotected control rod runout. Transient overpower tests on metallic and oxide fuels performed in Transient Reactor Test Facility (TREAT) have demonstrated a larger margin to cladding failure threshold for the metallic fuel. As shown in Fig. 8, oxide fuel pins fail typically 2.5 –3 times nominal peak power (4-4.5 times in adiabatic conditions), whereas metallic fuel pins fail 4-4.5 times nominal peak power.

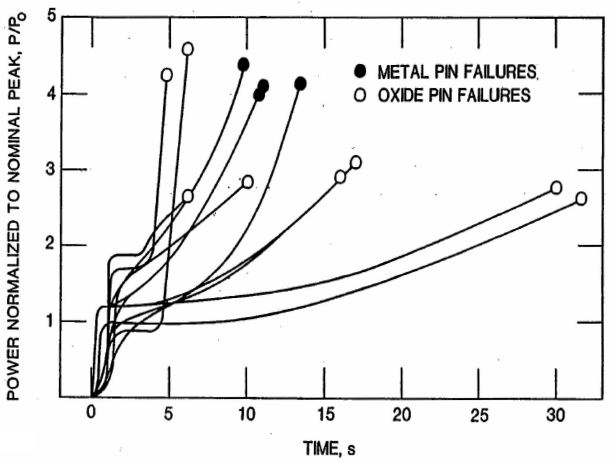

Fig. 8 Transient Overpower Failure Tests in TREAT Show Generally Greater Margins for Metallic Fuel

Another significant finding from these TREAT tests is that fission gas driven axial expansion of fuel within the cladding before failure provides an intrinsic and favorable negative reactivity feedback in the metallic fuel that has no parallel in oxide. The metallic fuel prefailure axial extrusion as a function of burnup is illustrated in Fig. 9.

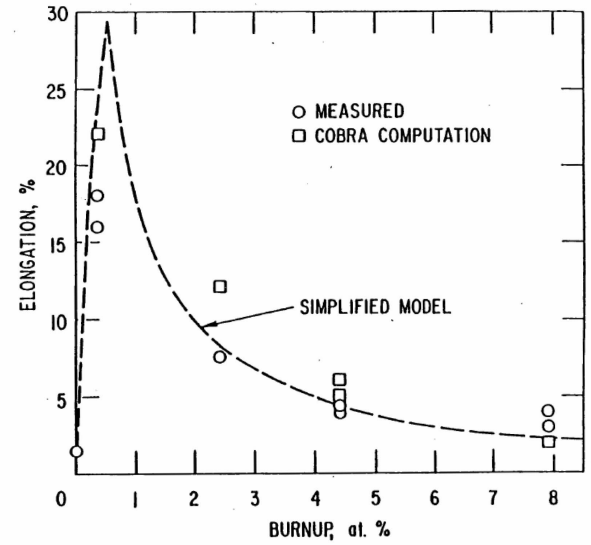

Fig. 9 Prefailure Axial Fuel Extrusion as a Function of Burnup for Metallic Fuel

5. FUEL CYCLE IMPLICATIONS

Metal fuel is easily fabricated using injection casting technique, requires no finishing, and allows a relaxed specification in dimensions and impurities that further simplifies the fabrication process. Furthermore, metal fuel is compatible with pyroprocessing based on electrorefining.

A pyrometallugical process was first utilized in recycling EBR-II metal fuel.[4] The spent fuel pins were mechanically de-clad to remove stainless steel cladding, and the fuel rods were chopped into small segments and loaded into a zirconia crucible where it was melted at 1400°C. The volatile fission products were collected in a fume trap, reactive metal fission products reacted with zirconia crucible wall to form oxide skull, and the molten metal was poured into a graphite mold and refabricated in an injection casting furnace. About 35,000 fuel pins had been recycled with a typical turnaround time of 50 days in the EBR-II Fuel Cycle Facility during the period of 1965 through 1969. This simple melt-refining process could not remove noble metal fission products, which was acceptable when the metal fuel achieved only about 1 % burnup. Since then the metal fuel performance has been improved to achieve greater than 15 % burnup, and hence the early process is inadequate. Furthermore, it did not have a provision for recovering actinides for recycle.

Therefore, in the Integral Fast Reactor (IFR) concept, a new pyroprocessing based on electrorefining was adopted in conjunction with the metallic fuel choice.[9-10] Metal fuel is a key factor in achieving compact and simple pyroprocessing, which utilizes high temperature, molten salt and metal solvents. Metal is both a suitable feed for such processes and the product as well, suitable for fabrication into new fuel pins.

Electrorefing is commonly utilized in the minerals industry to purify metals, such as aluminum and zinc. In pyroprocessing, electrorefining is the key step allowing the valuable fuel constituents, uranium and actinides, to be recovered and the fission products to be removed. A schematic of electrorefining is illustrated in Fig. 10. An electrorefiner, typically one meter in diameter, consists of an anode and a cathode submerged in molten electrolyte salt such as LiCl-KCl eutectic which has a low (350°C) melting point to allow operation at 500°C.

Following disassembly of the fuel assemblies, the fuel pins are chopped into short lengths, loaded into perforated steel baskets, and introduced into the electrorefiner as an anode. When a direct current is passed at low voltage (typically of the order of one volt) from anode to cathode, the bulk of the current passes through the electrolyte salt as uranium and actinide ions, which are reduced and collected at the cathode as metals. In other words, uranium and actinides are oxidized anodically in a molten salt electrolysis cell and deposited cathodically as solids.

There are two different cathodes. When current is passed, uranium dissolved in the electrolyte salt is deposited in the solid cathode. Actinides are also in solution, but the presence of uranium chloride in the electrolyte salt oxidizes actinide deposits back to chlorides. When the ratio of actinides to uranium reaches about two to three, then a liquid cadmium cathode is placed to collect all remaining uranium and actinides together. The formation of intermetallic compounds with Cd helps to retain actinides in the liquid Cd cathode. In order to avoid the distillation of a large amount of Cd, alternative actinide recovery processes are being developed at the present time, including a direct chemical reduction process using Li as reductant and an electrolytic reduction process.

There are two main waste products. The anode basket that contains the fuel cladding hulls and chemically noble fission products not dissolved during electrorefining is simply melted to form an exceptionally corrosion-resistant alloy. The metal waste form consists of primarily stainless steel and 15% zirconium as the base matrix.

Rare earth and active fission products as well as any excess salt are stabilized in the ceramic waste, a glass-bonded sodalite waste form. The actinides also form chlorides in the electrorefiner, so to minimize their loss, they are removed from the salt in a “drawdown” operation prior to salt purification. Molten alloys containing a reducing agent such as lithium are contacted with salt to reduce the actinides from the salt phase to the metal phase. The process is reversed to charge the next salt batch. After actinide removal, the salt is contacted with zeolite to remove fission products. The salt is then recycled. The salt-loaded zeolite is eventually combined with additional zeolite and 25% glass and processed thermally into a

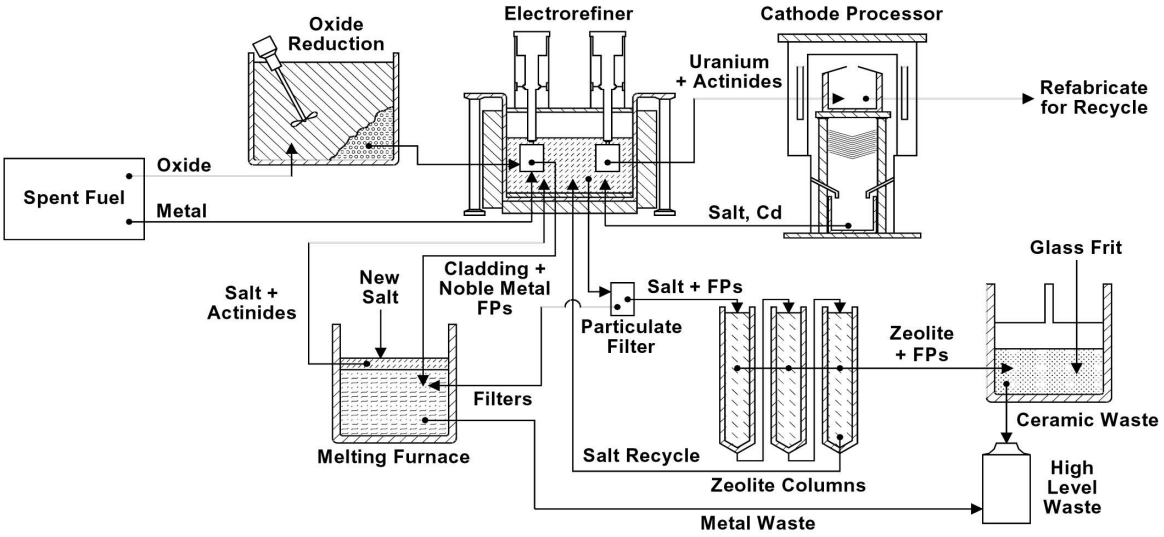

Fig. 10 Pyroprocessing Flowsheet

monolithic waste form. In this process, the zeolite is converted to sodalite, a stable naturally occurring mineral.

In pyroprocessing, all reagents such as electrolyte salts are recycled and there are no large volume low-level process waste streams. Secondary waste from pyroprocessing include operational wastes such as failed equipment, rags, packaging materials, dross, mold-scrap from fuel fabrication, and other miscellaneous items. These waste streams are categorized using existing orders or regulations and disposed of under standard practices. Items unique to pyroprocessing, like dross and mold-scrap from fuel casting, will undergo further treatment to recover actinides for recycle.

Much of the pyroprocessing technology was successfully demonstrated at Argonne-West as part of the three year (between 1996 and 1999) demonstration project treating 100 EBR-II driver fuel assemblies and 18 blanket assemblies. A special committee of the National Academy of Sciences found that this demonstration project met all criteria for success, and the Department of Energy followed with a formal decision to use this technology to treat the remaining 25 metric tons of EBR-II spent fuel. At the present time the pyroprocessing is being carried out at an engineering scale of about 50 kg batch operations. This represents a full scale for a fast reactor application, where the criticality concern limits the batch size.

6. SUMMARY AND CONCLUSIONS

Metal fuel has excellent steady-state irradiation performance characteristics if enough space is provided to form inter-connected porosity allowing fission gas release to the plenum. It has demonstrated a high burnup capability beyond 20%. Metal fuel also has superior off-normal performance characteristics, in particular for the run-beyond-cladding-breach conditions due to the compatibility of metal fuel with sodium coolant.

However, it is in the inherent passive safety potential where metal fuel is far superior to other fuel types. Due to low fuel operating temperature, the stored Doppler reactivity at power is small, which is an important factor for achieving benign responses to severe accident conditions. In addition, the vapor pressure of the bond sodium imbedded in the fuel porosity provides an axial fuel expansion force, resulting in a significant negative reactivity feedback prior to the cladding failure.

Metal fuel also allows a very simple injection-casting fabrication technique and electrorefining-based fuel cycle closure, which promises simpler waste management, proliferation-resistance, and much improved economics.

ACKNOWLEDGMENTS

This work was performed under the auspices of the U. S. Department of Energy under contract DE-AC02-06CH11357.

REFERENCES

[1] L. C. Walters, B. R. Seidel and J. H. Kittel, “Performance of Metallic Fuels and Blankets in Liquid-metal Fast Breeder Reactors,” *Nucl. Technol.* **65**[2], 179 (1984).
[2] B. R. Seidel, L. C. Walters and Y. I. Chang, “Advances in Metallic Nuclear Fuel,” *J. Metals*, **39**[4], 10 (1987).
[3] G. L. Hofman and L. C. Walters, “Metallic Fast Reactor

Fuels," in *Material Science and Technology: A Comprehensive Treatment*, R. W. Cahn, P. Haasen, and E. J. Kramer, eds., **10A** (1994).
[4] Charles E. Stevenson, *The EBR-II Fuel Cycle Story*, American Nuclear Society (1987).
[5] C. E. Till and Y. I. Chang, "The Integral Fast Reactor," in *Advances in Nuclear Science and Technology*, **20**, 127 (1988).
[6] Y. I. Chang, "The Integral Fast Reactor," *Nucl. Technol.* **88**[11], 129 (1989).
[7] S. H. Fistedis, ed., *The Experimental Breeder Reactor-II Inherent Safety Demonstration*, North-Holland (1987): reprinted from *Nuclear Engineering and Design*, **101**[1] (1987).
[8] D. C. Wade and Y. I. Chang, "The Integral Fast Reactor Concept: Physics of Operation and Safety," *Nucl. Sci. and Eng.* **100**, 507 (1988).
[9] L. Burris, R. K. Steunenberg, and W. E. Miller, "The Application of Electrorefining fpr Recovery and Purification of Fuel from the Integral Fast Reactor," Proc. *Annual AIChE Meeting*, Miami, Florida, November 2-7, 1986.
[10] Y. I. Chang, "Advanced Nuclear Energy System for the Twenty-First Century," *Proc. Int. Conf. New Frontiers of Nuclear Technology: Reactor Physics (PHYSOR 2002)*, Seoul, Korea, Oct. 7-10, 2002.